Neurobiology of Disease 157 (2021) 105443

Contents lists available at ScienceDirect

Neurobiology of Disease

journal homepage: www.elsevier.com/locate/ynbdi

Targeted overexpression of glutamate transporter-1 reduces seizures and attenuates pathological changes in a mouse model of epilepsy

Allison R. Peterson [a], Terese A. Garcia [a], Kyle Cullion [b], Seema K. Tiwari-Woodruff [a], Ernest V. Pedapati [b,c], Devin K. Binder [a,*]

[a] Division of Biomedical Sciences, Center for Glial-Neuronal Interactions, School of Medicine, University of California, Riverside, CA, USA
[b] Division of Child and Adolescent Psychiatry, Cincinnati Children's Hospital Medical Center, Cincinnati, OH, USA
[c] Division of Neurology, Cincinnati Children's Hospital Medical Center, Cincinnati, OH, USA

ARTICLE INFO

Keywords:
Epilepsy
Glutamate transporter-1
GLT-1
AAV
Kainic acid
Seizure
Astrocyte

ABSTRACT

Astrocytic glutamate transporters are crucial for glutamate homeostasis in the brain, and dysregulation of these transporters can contribute to the development of epilepsy. Glutamate transporter-1 (GLT-1) is responsible for the majority of glutamate uptake in the dorsal forebrain and has been shown to be reduced at epileptic foci in patients and preclinical models of temporal lobe epilepsy (TLE). Current antiepileptic drugs (AEDs) work primarily by targeting neurons directly through suppression of excitatory neurotransmission or enhancement of inhibitory neurotransmission, which can lead to both behavioral and psychiatric side effects. This study investigates the therapeutic capacity of astrocyte-specific AAV-mediated GLT-1 expression in the intrahippocampal kainic acid (IHKA) model of TLE. In this study, we used Western blot analysis, immunohistochemistry, and long-term-video EEG monitoring to demonstrate that cell-type-specific upregulation of GLT-1 in astrocytes is neuroprotective at early time points during epileptogenesis, reduces seizure frequency and total time spent in seizures, and eliminates large behavioral seizures in the IHKA model of epilepsy. Our findings suggest that targeting glutamate uptake is a promising therapeutic strategy for the treatment of epilepsy.

1. Introduction

Epilepsy is a disorder of the brain characterized by unprovoked seizures (Fisher et al., 2014). There are more than 3 million cases of active epilepsy in the United States, making it one of the most common disorders of the nervous system (Zack and Kobau, 2017). Temporal lobe epilepsy (TLE) is the most common form of epilepsy with focal seizures. TLE is also frequently associated with refractory epilepsy. It is estimated that 143,000–191,000 US patients still suffer from refractory TLE that cannot be controlled with current AEDs (Asadi-Pooya et al., 2017).

Current AEDs work primarily by targeting neurons through direct modulation of neurotransmission by inhibition of glutamatergic excitatory neurotransmission or enhancement of GABAergic inhibitory neurotransmission. Modulation of neurotransmission can consequently lead to "neurotoxic" adverse effects (*e.g.* drowsiness, incoordination, fatigue, cognitive impairment), which are common undesired effects associated with AED usage (Park and Kwon, 2008). Studies have shown that short-term use of AEDs can damage neurons, and combined use of multiple AEDs can exacerbate this damage (Liu et al., 2015). Adverse effects of AEDs can also lead to poor adherence and AED discontinuation in up to 30% of patients (Bootsma et al., 2009).

Therefore, non-neuronal targets are an attractive alternative approach to treat epilepsy with potentially fewer deleterious effects (Binder, 2018). Increasing evidence suggests that changes in astrocytes can contribute to the development of epilepsy (Eid et al., 2004; Fedele et al., 2005; Heuser et al., 2018; Hinterkeuser et al., 2000; Ivens et al., 2007). Astrocytes play an essential role in ionic homeostasis, neurotransmitter clearance, and potassium buffering in the central nervous system (CNS). Due to their close association with synapses, astrocytes can alter synaptic function and are the key players in extracellular

Abbreviations: AEDs, Antiepileptic drugs; AAV, Adeno-associated virus; CNS, Central nervous system; DAPI, 4′,6-diamidino-2-phenylindole; EEG, Electroencephalogram; GFAP, Glial fibrillary acidic protein; GLT-1, Glutamate transporter-1; GCL, Granule cell layer; IHKA, Intrahippocampal kainic acid; SE, Status epilepticus; TLE, Temporal lobe epilepsy.

* Corresponding author at: Division of Biomedical Sciences, University of California, Riverside, 2120 Multidisciplinary Research Building, Riverside, CA 92521, USA.
E-mail address: dbinder@ucr.edu (D.K. Binder).

https://doi.org/10.1016/j.nbd.2021.105443
Received 7 May 2021; Received in revised form 2 July 2021; Accepted 5 July 2021
Available online 9 July 2021

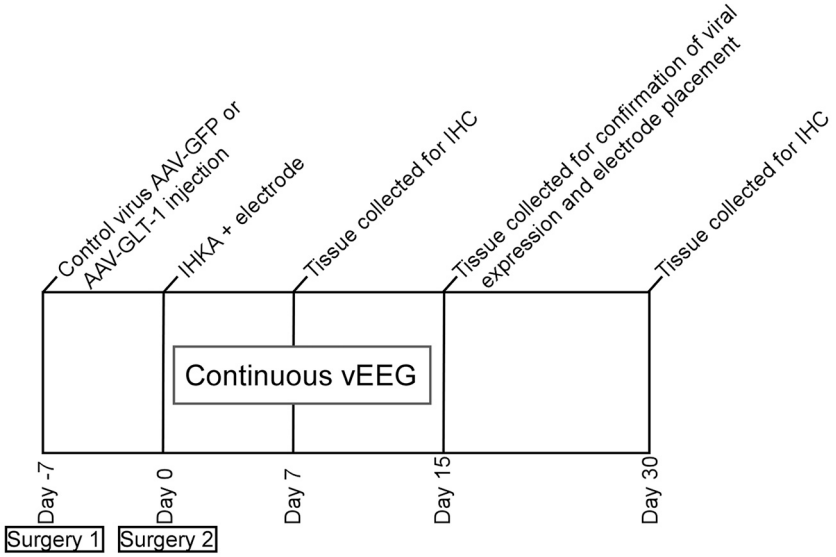

Fig. 1. Overview of experimental design. Mice were unilaterally infused with control virus AAV-GFP or AAV-GLT-1 into the dorsal hippocampus. One week following AAV infusion mice were injected with kainic acid into the ipsilateral hippocampus to induce status epilepticus. A subset of mice were implanted with a bipolar twist electrode for continuous video EEG monitoring. Tissue was collected at 7 and 14 days post-IHKA for immunohistochemistry.

glutamate homeostasis in the CNS. Extracellular glutamate levels must be tightly regulated to maintain proper neuronal activity and function. Glutamate transporters are responsible for removing glutamate from the extracellular space following neurotransmitter release into the synaptic cleft. Glutamate transporter-1 (GLT-1) is responsible for approximately 90% of the total glutamate clearance from the synaptic cleft and is essential for maintaining low levels of extracellular glutamate (Danbolt, 2001). Glutamate transporters have been shown to be reduced in resected human epilepsy tissue and in preclinical models of TLE (Hubbard et al., 2016; Mathern et al., 1999; Peterson and Binder, 2019b; Peterson and Binder, 2020; Tessler et al., 1999). Recently, *de novo* mutations in glutamate transporters, particularly GLT-1, have been identified in patients and families with early-onset multiple seizure types (Consortium, 2016). Perisynaptic GLT-1 protein levels are downregulated at a critical time point in epileptogenesis, suggesting that GLT-1 dysregulation could contribute to the development of epilepsy (Clarkson et al., 2020; Peterson and Binder, 2019b). GLT-1 global KO mice die from spontaneous seizures (Tanaka et al., 1997); in contrast, transgenic mice that overexpress GLT-1 have a higher seizure threshold than wild-type mice, suggesting that GLT-1 plays an essential role in seizure generation and protection against glutamate toxicity (Kong et al., 2012). Deletion of GLT-1 specifically in astrocytes leads to uncontrolled seizures and excess mortality at an early age, suggesting that astrocytic GLT-1-mediated glutamate uptake is essential to protect against fatal epilepsy (Petr et al., 2015).

Therefore, strategies to upregulate GLT-1 would be expected to be neuroprotective in various neurological models. Focal overexpression of GLT-1 using an adeno-associated virus (AAV)-GLT-1 viral vector reduces ischemia-induced glutamate overflow, decreases cell death, and improves behavioral outcome in a preclinical model of stroke (Harvey et al., 2011). Intraspinal AAV-GLT-1 delivery has also been shown to attenuate heat hypersensitivity following cervical contusion spinal cord injury (SCI) (Falnikar et al., 2016). Here we develop and employ an AAV8-Gfa2-GLT-1-cHA viral vector to promote cell-type-specific GLT-1 transcription under the glial fibrillary acid protein (GFAP) promoter in the intrahippocampal kainic acid (IHKA) model of epilepsy. We demonstrate that treatment with AAV8-Gfa2-GLT-1-cHA delays neuronal cell loss, decreases dentate cell dispersion and suppresses seizure activity.

2. Materials and methods

2.1. Animals

8–10-week-old Charles River CD1 male mice were housed under a 12-h light and 12-h dark cycle with *ad libitum* access to food and water. All experiments performed were approved by the University of California, Riverside Institutional Animal Care and Use Committee (IACUC) and were conducted in accordance with the National Institutes of Health (NIH) guidelines. A total of 58 animals were used for this study.

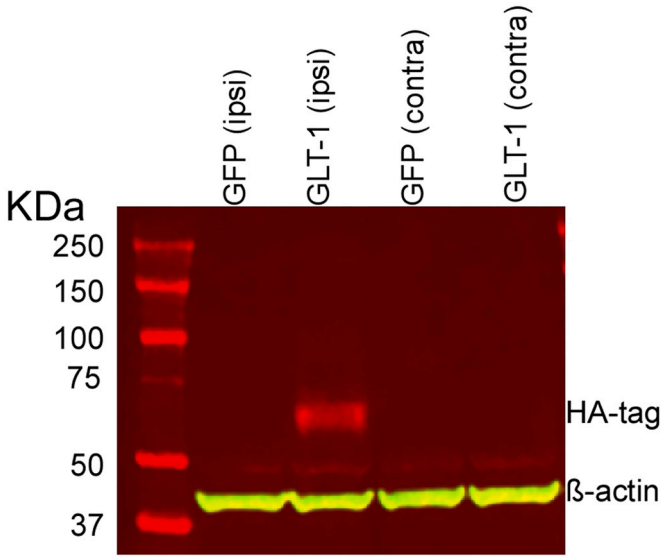

Fig. 2. Representative western blot of HA-tagged GLT-1 expression in the hippocampus 14 days post-AAV injection. From left to right, Lane 1 shows absence of HA-tagged GLT-1 in the ipsilateral hippocampus of AAV-GFP injected mice, Lane 2 shows expression of HA-tagged GLT-1 in the ipsilateral hippocampus of AAV-GLT-1-cHA injected mice, Lane 3 shows absence of HA-tagged GLT-1 in the contralateral hippocampus of AAV-GFP injected mice, Lane 4 shows absence of HA-tagged GLT-1 in the contralateral hippocampus of AAV-GLT-1-cHA injected mice.

2.2. Study design

Animals were injected with the control virus AAV8-Gfa2-GFP or AAV8-Gfa2-GLT-1-cHA into the dorsal hippocampus one week prior to intrahippocampal kainic acid-induced status epilepticus. One week following AAV8 administration, kainic acid was microinjected into the same hippocampal location to induce SE. To evaluate immunohistological changes between the animals injected with the control virus AAV-Gfa2-GFP and the animals that received AAV-Gfa2-GLT-1-cHA a subset of animals were collected at 7 and 30 days post-IHKA induced SE. A cohort of animals was implanted with an electrode in the ipsilateral hippocampus immediately following kainic acid injection and underwent vEEG recordings for two weeks to compare epileptiform activity between animals injected with the control virus AAV-Gfa2-GFP and animals injected with AAV8-Gfa2-GLT-1-cHA (Fig. 1).

2.3. AAV8 intrahippocampal injection

Mice were anesthetized with a solution of ketamine (80 mg/kg)/xylazine (10 mg/kg) and positioned in a stereotaxic frame. The skull was exposed, bregma was located, and a craniotomy was performed 1.8 mm posterior and 1.6 mm lateral to bregma. 1.5 μl AAV8-Gfa2-GLT-1-cHA vector (titer of 10^{13} genomic particles/ml) was injected using a Hamilton syringe at 0.2 μl/min over 8 min. When the injection was finished, the pipette was left in place for 3 min to prevent efflux of the virus during pipette removal. Age-matched controls were injected with AAV8-Gfa2-GFP vector (titer of 10^{13} genomic particles/ml) (control).

2.4. IHKA-induced status epilepticus and electrode implantation

One week following AAV injections, IHKA injections were used to induce epileptogenesis, as previously described (Hubbard et al., 2016; Lee et al., 2012; Peterson and Binder, 2019b). Mice were anesthetized with a solution of ketamine (80 mg/kg)/xylazine (10 mg/kg) and positioned in a stereotaxic frame. The skull was exposed, bregma was located, and a craniotomy was performed 1.8 mm posterior and 1.6 mm lateral to bregma. Mice were injected with 64 nl of 20 mM kainic acid (Tocris) using a microinjector (Nanoject II, Drummond Scientific) into the CA1 region of the dorsal hippocampus (lowered to 1.9 mm dorsoventral). In a subset of mice, immediately following KA injection the syringe was withdrawn and a 3 channel two twisted stainless-steel electrode (Plastics One) was implanted into the dorsal hippocampus. The twisted bipolar wires, 2 mm length, were implanted into the dorsal hippocampus (lowered to 1.9 mm dorsoventral) and the untwisted wire was cut to ground the surface of the cortex. Dental cement was used to secure the electrode in place (Panavia SA cement). Following injections, mice experienced status epilepticus, defined by Racine scale stage 3–5 seizures (Racine, 1972) for at least 3 h. The presence of epileptiform activity and the development of spontaneous seizures has previously been confirmed by chronic video-EEG recordings to occur in 100% of animals after IHKA injections (Lee et al., 2012). We monitored mice for 5 h following IHKA injection using video recording to verify the presence of Racine stage 3–5 seizures. All animals included in this study experienced continuous SE, characterized by forelimb and hindlimb clonus, rearing, jumping, and falling (Racine, 1972). We observed SE in both AAV-GFP and AAV-GLT-1 treatment groups, with no difference in

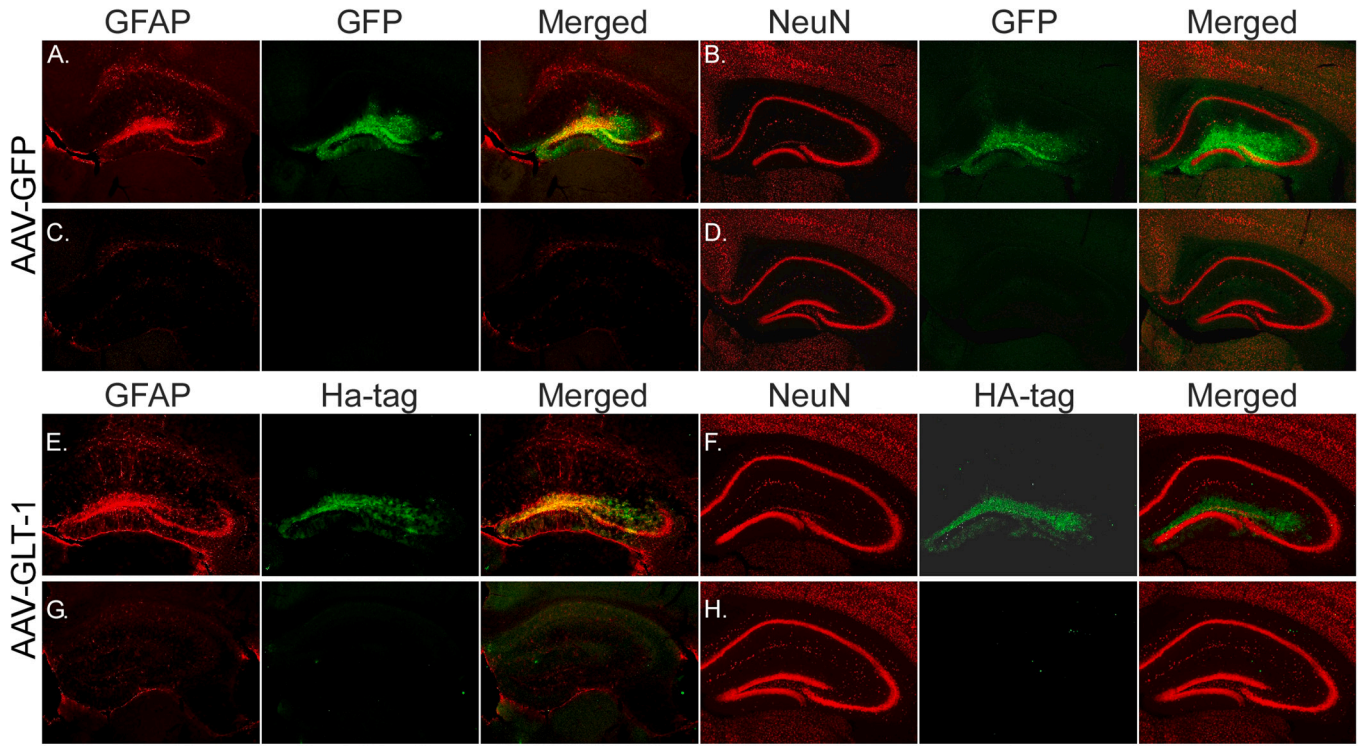

Fig. 3. AAV transduction in the mouse hippocampus 12 days post-injection. A. Coronal section of the ipsilateral hippocampus showing expression of GFAP (red) and GFP (green) following AAV-GFP injection. B. Coronal section of the ipsilateral hippocampus showing expression of NeuN (red) and GFP (green) following AAV-GFP injection. C. Coronal section of the contralateral hippocampus showing expression of GFAP (red) and GFP (green) following AAV-GFP injection. D. Coronal section of the contralateral hippocampus showing expression of NeuN (red) and GFP (green) following AAV-GFP injection. E. Coronal section of the ipsilateral hippocampus showing expression of GFAP (red) and HA-tag (green) following AAV-GLT-1-cHA injection. F. Coronal section of the ipsilateral hippocampus showing expression of NeuN (red) and HA-tag (green) following AAV-GLT1-cHA injection. G. Coronal section of the contralateral hippocampus showing expression of GFAP (red) and HA-tag (green) following AAV-GLT-1-cHA injection. D. Coronal section of the contralateral hippocampus showing expression of NeuN (red) and GFP (green) following AAV-GLT1-cHA injection. $N = 8$ section per group (4 animals per group) (5×). (For interpretation of the references to colour in this figure legend, the reader is referred to the web version of this article.)

duration, but mortality was slightly reduced in mice pretreated with AAV-GLT1. For the AAV-GFP pretreated group, mortality during the initial SE was 18%, while mortality in the AAV-GLT-1 pretreated group was 13%. Animals that died due to SE were excluded from the study. Electrode placement and viral expression was confirmed in all mice. Mice were excluded from the study when hippocampal viral expression could not be confirmed (GFP expression was used for mice injected with AAV-Gfa2-GFP and HA-tag expression was used for mice injected with AAV-Gfa2-GLT-1-cHA) or when electrode placement was not in the hippocampus.

2.5. Continuous video-EEG acquisition

Video-EEG acquisition began immediately following surgery and continued for 14 days. Mice were recorded using a tethered system (BIOPAC MP150) and a commutator which allowed freedom of motion. EEG output was amplified with a gain of 5000 and digitized at a sampling rate of 1250 Hz.

2.6. Electrographic seizure analysis

Acquired EEG files were post-processed with bandpass filter from 0.1 to 60 Hz. Electrographic seizures were quantified using an automated algorithm set to customized parameters for each subject. Customized

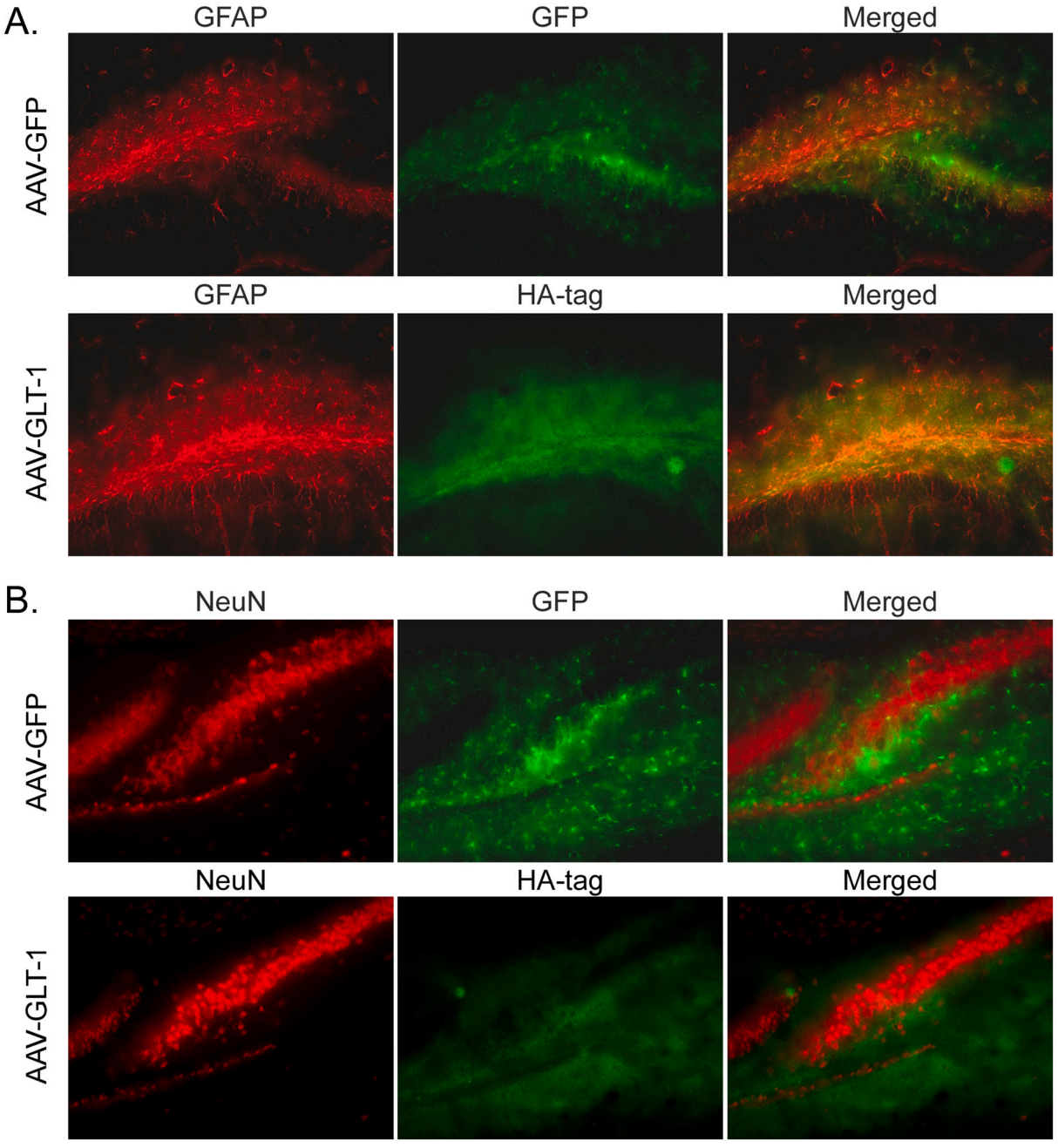

Fig. 4. Cell-type specific AAV transduction in the dentate gyrus 12 days post-injection. A. Coronal section of the ipsilateral hippocampus showing expression of GFAP (red), GFP (green) and HA-tag (green) following AAV injection. B. Coronal section of the ipsilateral hippocampus showing expression of NeuN (red), GFP (green) and HA-tag (green) following AAV injection. $N = 8$ sections per group (4 animals per group) (20×). (For interpretation of the references to colour in this figure legend, the reader is referred to the web version of this article.)

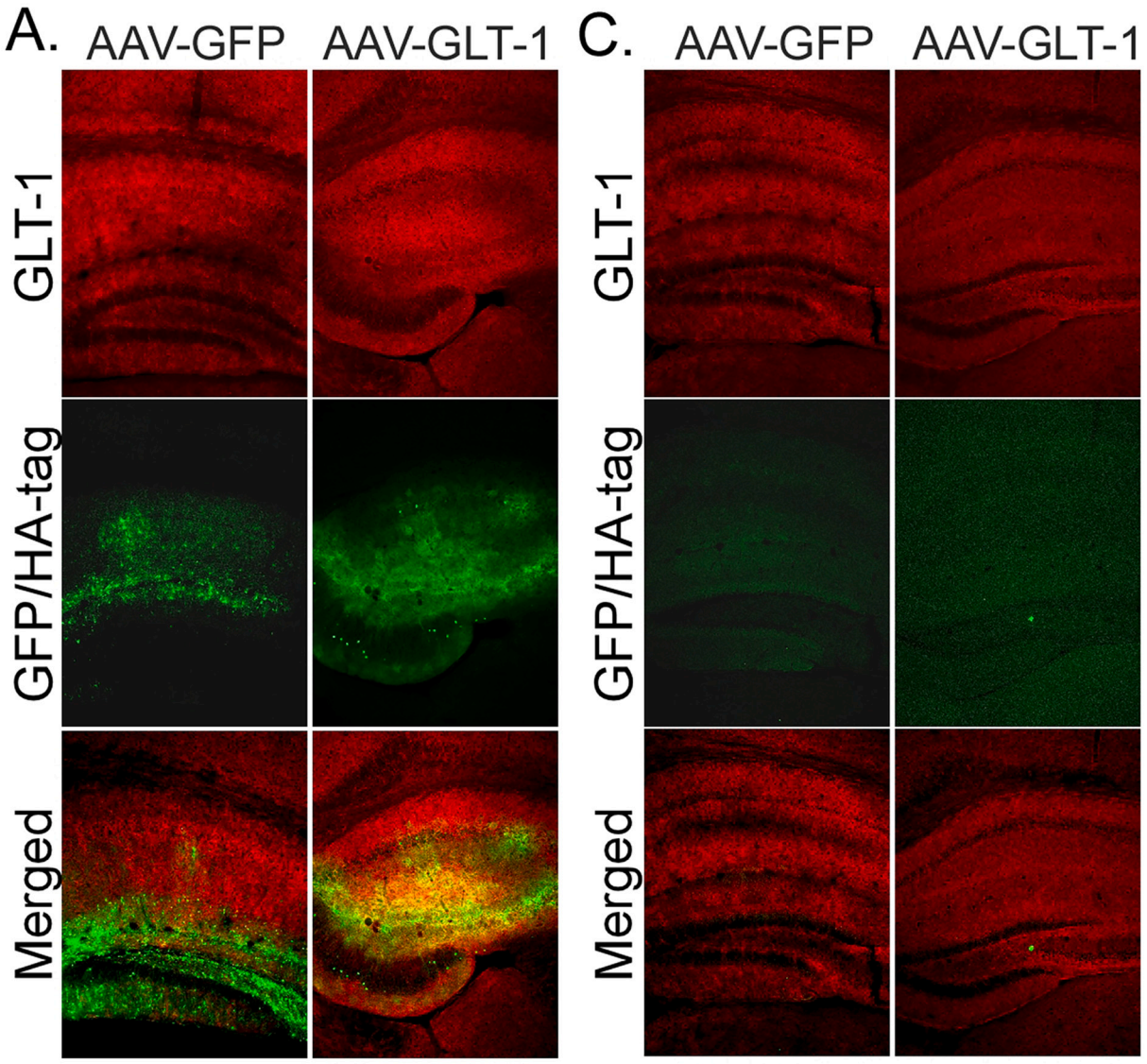

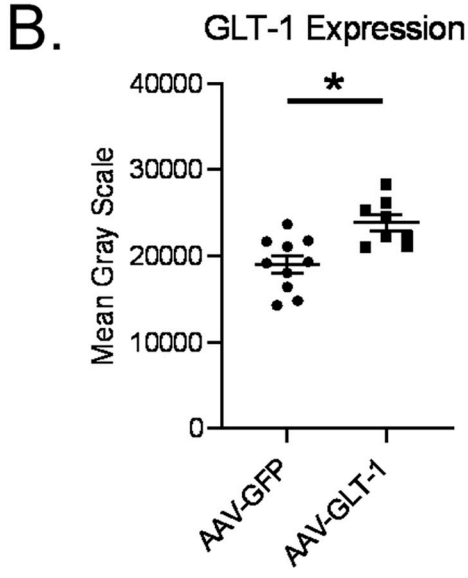

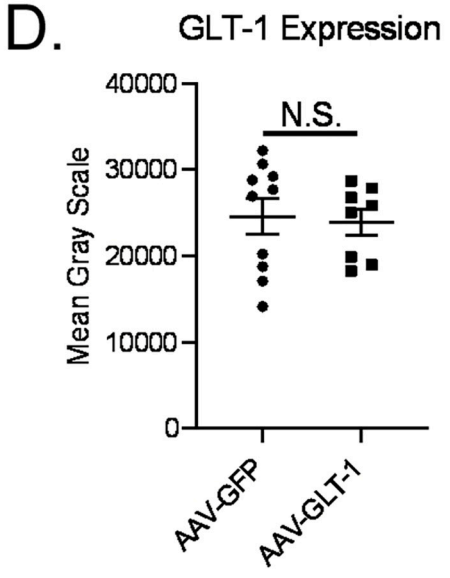

(caption on next page)

Fig. 5. GLT-1 expression is increased in AAV pretreated mice in the ipsilateral hippocampus 7 days post-kainate induced status epilepticus. A. Coronal section of the ipsilateral hippocampus 7 days post-kainate induced status epilepticus showing expression of GLT-1 (red), GFP/HA-tag (green) following AAV injection. B. Mean gray scale quantitation of total hippocampus GLT-1 expression in the ipsilateral hippocampus 7 days post-kainate induces status epilepticus. C. Coronal section of the contralateral hippocampus 7 days post-kainate induced status epilepticus showing expression of GLT-1 (red), GFP/HA-tag (green) following AAV injection. D. Mean gray scale quantitation of total hippocampus GLT-1 expression in the contralateral hippocampus 7 days post-kainate induces status epilepticus. AAV-GFP group; $N = 11$ sections (6 animals). AAV-GLT-1 group; $N = 8$ sections (5 animals) (5×) . (For interpretation of the references to colour in this figure legend, the reader is referred to the web version of this article.)

parameters were based on the mean amplitude of the hippocampal recordings, ictal spike width, and time between spikes. Automated electrographic seizure analysis software used was modified and extended with an expanded graphical user interface (GUI) from a previously published and validated MATLAB algorithm (Zeidler et al., 2018). For all animals, a seizure was defined as at least 3 spikes of greater than twice the baseline amplitude within each 1 s bin (3 Hz). Interictal periods were set at a minimum of 5 s. All electrographic seizure-like events detected were visually inspected for false positives. Events that contained noise were further confirmed with video verification. All events detected that were ≥ 20 s were further examined with video to determine presence of large behavioral seizures (LBSs). Large behavioral seizures were defined at ≥3 on the Racine scale (Racine, 1972). All electrographic seizure analysis was performed blinded to experimental group.

2.7. Code accessibility

The codebase used is an expanded version of the previously published and validated algorithm (Zeidler et al., 2018), along with utilization of version 13.6.5b of the EEGLAB MATLAB library published by University of California San Diego (UCSD), to include an updated graphical user interface (GUI). The added features include custom channel selection for necessary analysis with visualization of up to 4 channels' time series at a time, manual threshold adjustment per channel, significant speedup for calculations and detection *via* the MATLAB parallel processing toolbox, and user-defined selection and separation between true events, non-events, events containing noise, and possible short events *via* visual inspection for each corresponding window of data in the time series. The graphical user interface (GUI) and underlying code are freely accessible online at the following public repository: https://github.com/eplab1745/ESA_Extended.

2.8. Western blot analysis

Total protein concentrations of homogenized hippocampal tissue samples were obtained using a Bradford assay. Protein was resolved by sodium dodecyl sulfate polyacrylamide gel electrophoresis (SDS-PAGE) using 10% polyacrylamide gels and then transferred to a nitrocellulose membrane. Following transfer, membranes were briefly rinsed with TBS and blocked for 1 h in 5% milk in Tris-buffered saline 0.1% Tween 20 (Sigma) at room temperature (RT). Membranes containing AAV-Gfa2-GFP and AAV-Gfa2-GLT-1-cHA-injected samples were then probed for Hemagglutinin-tag (1:200, Novus Biologicals N600–362) and β-actin (1:10,000, Sigma A1978). Bands were visualized and quantified using species specific antibodies (IRDye; LI-COR) and the LI-COR Odyssey Fc Western Imaging System.

2.9. Immunohistochemistry

Mice were euthanized with Fatal Plus (Western Medical Supply) then perfused with ice-cold phosphate buffered saline (PBS) followed by 4% paraformaldehyde (PFA). Brains were harvested and fixed in 4% PFA for two hours at 4 °C. Harvested brains were then dehydrated in 30% sucrose and stored at 4 °C until use. Prior to sectioning, harvested brains were flash frozen with ice-cold isopentane. Frozen brains were sealed in optimum cutting temperature (OCT) formulation at 20 °C and sliced into 50 μm sections using a cryostat. Sections were stored in 0.01% sodium azide PBS at 4 °C.

For *in vivo* AAV transduction experiments to verify transduction and cell-type specificity of the virus, brains were harvested 12 days post AAV-injection. $N = 8$ sections per group were analyzed (4 animals per group). For AAV-pretreated mice, brains were harvested 7 and 30 days post-IHKA-induced SE. For each animal, per stain, two sections were processed for immunohistochemistry, 1 ventral and 1 dorsal to the injection site. For immunohistochemistry, sections were washed with PBST, permeabilized with 0.5% Tween 20 for 30 min at room temperature (RT), then blocked for 1 h at RT with 10% bovine serum albumin. Sections were then incubated 1.5 h at RT in 0.5% Tween-20/5% BSA with primary antibodies to Hemagglutinin-tag (1:200, Novus Biologicals N600–362), GFAP (1:500, Abcam ab7260), NeuN (1:200, EMD Millipore ABN78) and GLT-1 (1:400, cGLT1a antibody generously provided by Dr. Jeff Rothstein). Sections were washed with PBS and incubated with Alexa 594 (Molecular Probes/Invitrogen), Alexa 488, and Alexa 647 (Molecular Probes/Invitrogen) for visualization and mounted in Vectashield with DAPI (Vector Laboratories).

2.10. Imaging and quantification

Hippocampal images were captured at 5×, 10×, and 20× magnification using a fluorescence microscope (Leica DFC345FX) under identical settings for each channel. Quantification was performed using ImageJ software. For NeuN immunoreactivity quantification, mean gray value was calculated across the entire image for each region of interest: S. pyramidale of CA1, S. pyramidale of CA3, and dentate gyrus. For granule cell width measurements, the width of the widest point of the central two-thirds of the outer blade of the dentate gyrus ipsilateral to injection was measured and normalized to the contralateral hippocampus measurements from the same section. Granule cell width measurements were performed blinded to experimental group. For GLT-1 quantitation at 7 and 30 days post-IHKA-induced status epilepticus, region of interest (ROI)-based analysis was standardized by drawing a large box including CA1, DG and CA3 to denote total hippocampal immunoreactivity using the DAPI channel. This ROI was then used to measure mean gray value for GLT-1 . Confocal imaging (Supplemental Fig. S1) was performed with an Olympus BX61 confocal microscope (Olympus America Inc., Center Valley, PA).

2.11. Statistical analysis

Statistical analysis was performed using Prism 8 software (GraphPad Software, La Jolla, CA). All datasets were analyzed using an unpaired one-tailed *t*-test with a 95% confidence interval (CI) except for large behavioral seizures (LBSs). LBSs were analyzed using a Mann-Whitney *U* test with a 95% confidence interval (CI). All error bars are presented as the mean ± standard error of the mean (SEM). Difference between groups was considered statistically significant by a *P*-value ≤0.05 and was denoted with one asterisk (*).

3. Results

3.1. Cell-type specific AAV transduction in the mouse hippocampus

Expression of exogenous GLT-1 protein *in vivo* was confirmed by

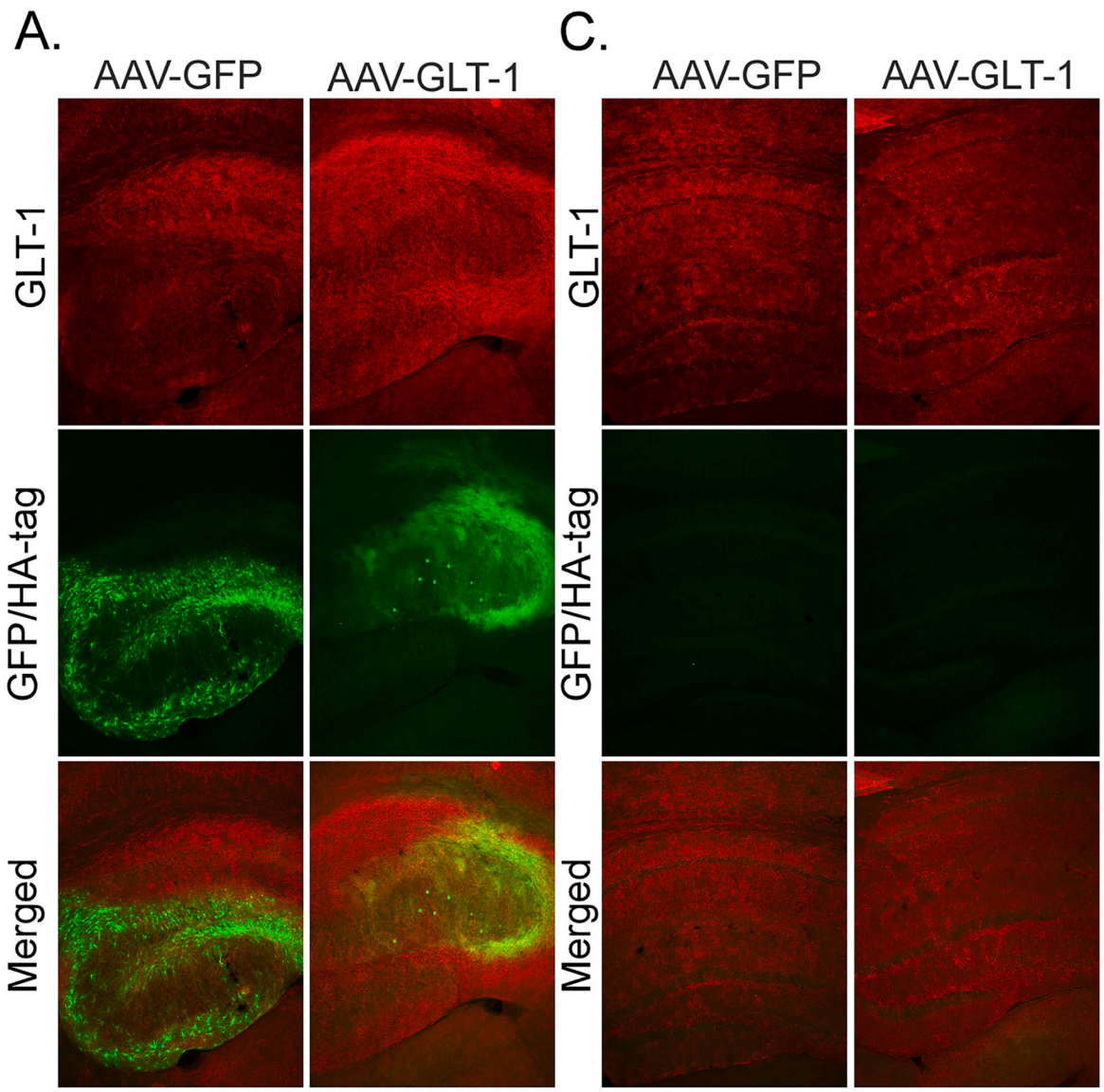

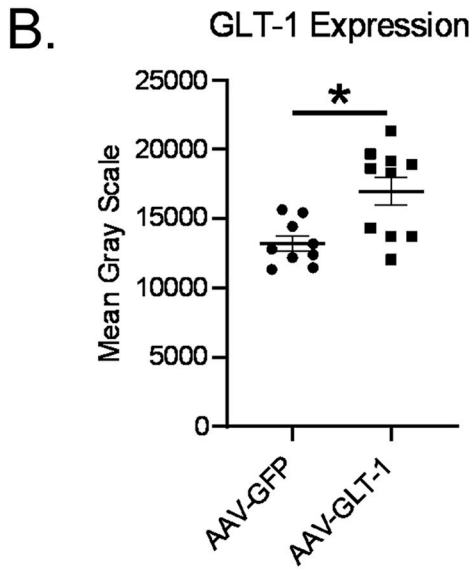

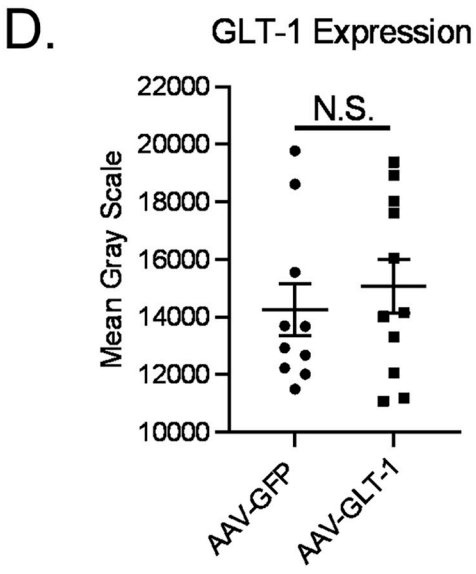

(caption on next page)

Fig. 6. GLT-1 expression is increased in AAV pretreated mice in the ipsilateral hippocampus 30 days post-kainate induced status epilepticus. A. Coronal section of the ipsilateral hippocampus 30 days post-kainate induced status epilepticus showing expression of GLT-1 (red), GFP/HA-tag (green) following AAV injection. B. Mean gray scale quantitation of total hippocampus GLT-1 expression in the ipsilateral hippocampus 30 days post-kainate induces status epilepticus. C. Coronal section of the contralateral hippocampus 30 days post-kainate induced status epilepticus showing expression of GLT-1 (red), GFP/HA-tag (green) following AAV injection. D. Mean gray scale quantitation of total hippocampus GLT-1 expression in the contralateral hippocampus 30 days post-kainate induces status epilepticus. AAV-GFP group; $N = 10$ sections (6 animals). AAV-GLT-1 group; $N = 11$ sections (6 animals) (5×). (For interpretation of the references to colour in this figure legend, the reader is referred to the web version of this article.)

probing for the HA-tag fused to GLT-1 protein. We found robust expression of HA-tagged GLT-1 in the ipsilateral hippocampus 14 days post-AAV-Gfa2-GLT-1-cHA injection compared to the hippocampus of mice injected with AAV-Gfa2-GFP (Fig. 2). We did not observe HA-tagged GLT-1 expression in the contralateral hippocampus of AAV-Gfa2-GLT-1-cHA injected mice (Fig. 2). Using immunohistochemistry, we determined that both AAV-Gfa2-GLT-1-cHA and AAV-Gfa2-GFP are expressed throughout the ipsilateral hippocampus 12 days post-injection (Fig. 3). Merged channels confirmed (shown in orange) HA-tagged GLT-1 is found in cells expressing GFAP and not in cells expressing the neuronal marker NeuN (Fig. 3, Fig. 4). HA-tagged GLT-1 expression observed was shown as puncta resembling astrocytic bush like-morphology (Supplemental Fig. S1).

3.2. Pretreatment with AAV-GLT1 increases GLT-1 expression during epileptogenesis

Hippocampal GLT-1 immunoreactivity was assessed at 7 and 30 days post-IHKA-induced SE in AAV-Gfa2-GFP and AAV-Gfa2-GLT-1-cHA pretreated mice. Quantitation of total hippocampal GLT-1 protein immunoreactivity was performed for both hippocampi ipsilateral and contralateral to injection at 7 (Fig. 5) and 30 (Fig. 6) days post-IHKA-induced SE. A one-tailed *t*-test on GLT-1 immunoreactivity in the ipsilateral hippocampus at 7 days post-IHKA revealed a main effect of treatment ($t(df) = 3.509(16)$, $p = 0.0015$; mean ± SEM: AAV-GFP = 19,034 ± 990.3; AAV-GLT-1 = 23,893 ± 926.8) (Fig. 5). A one-tailed t-test on GLT-1 immunoreactivity in the ipsilateral hippocampus at 30 days post-IHKA revealed a main effect of treatment ($t(df) = 3.179$ (19), $p = 0.0027$; mean ± SEM: AAV-GFP = 13,220 ± 538.2; AAV-GLT-1 = 16,988 ± 1013) (Fig. 6). A t-test on GLT-1 immunoreactivity in the contralateral hippocampus at 7 and 30 days post-IHKA revealed no effect of treatment ($p > 0.05$).

3.3. Pretreatment with AAV-GLT-1 is neuroprotective at early time points during the development of epilepsy

Hippocampal NeuN immunoreactivity was assessed at 7 and 30 days post-IHKA-induced SE in AAV-Gfa2-GFP and AAV-Gfa2-GLT-1-cHA pretreated mice. Quantification of NeuN-immunoreactive neurons was examined in S. pyramidale of CA1, S. pyramidale of CA3, and dentate gyrus for hippocampi both ipsilateral (Fig. 7, Fig. 9) and contralateral (Fig. 8, Fig. 10) to injection. A one-tailed *t*-test on NeuN immunoreactivity in S. pyramidale of CA1 of the ipsilateral hippocampus 7 days post-IHKA revealed no effect of treatment ($t(df) = 0.07913(22)$, $p = 0.4688$; mean ± SEM: AAV-GFP = 20.46 ± 0.9208; AAV-GLT-1 = 20.33 ± 1.284). A one-tailed t-test on NeuN immunoreactivity in S. pyramidale

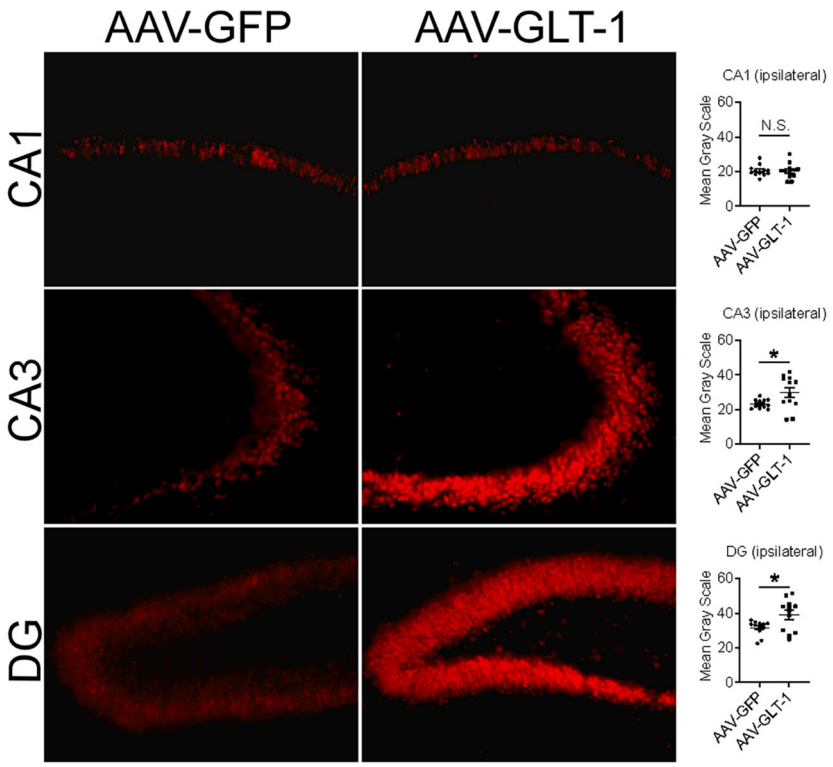

Fig. 7. NeuN expression in AAV pretreated mice in the ipsilateral hippocampus 7 days post-kainate induced status epilepticus. Coronal section of the ipsilateral hippocampus 7 days post-kainate induced status epilepticus showing expression and quantitation of NeuN immunoreactivity following AAV injection. $N = 12$ sections per group (6 animals per group) (20×).

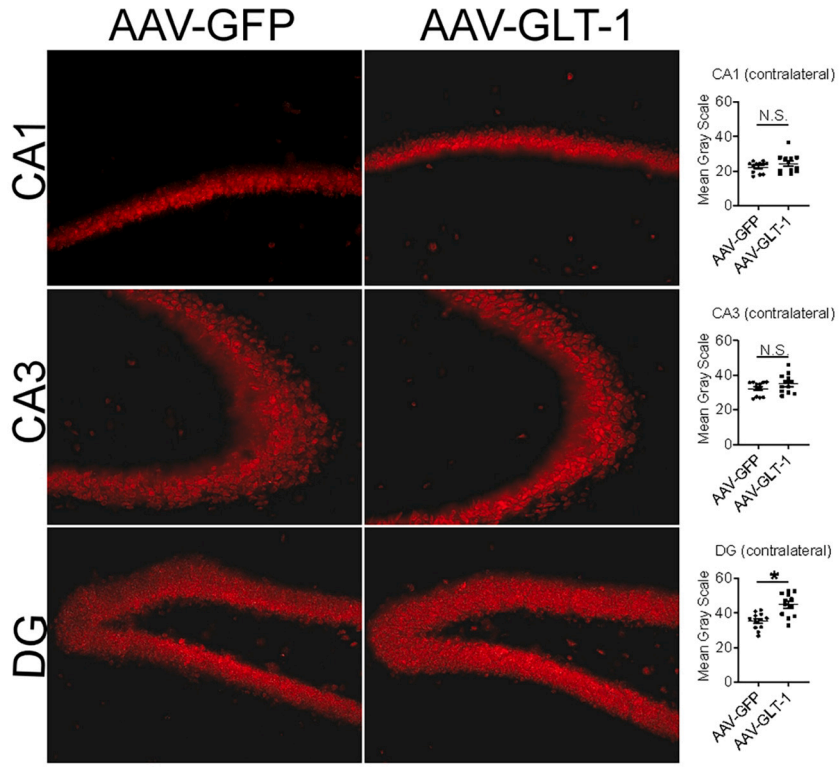

Fig. 8. NeuN expression in AAV pretreated mice in the contralateral hippocampus 7 days post-kainate induced status epilepticus. Coronal section of the contralateral hippocampus 7 days post-kainate induced status epilepticus showing expression and quantitation of NeuN immunoreactivity following AAV injection. $N = 12$ sections per group (6 animals per group) (20×).

of CA3 in the ipsilateral hippocampus 7 days post-IHKA revealed a main effect of treatment (t(df) = 2.335(22), $p = 0.0145$; mean ± SEM: AAV-GFP = 23.24 ± 0.7344; AAV-GLT-1 = 29.93 ± 2.773). A one-tailed t-test on NeuN immunoreactivity in the dentate gyrus of the ipsilateral hippocampus 7 days post-IHKA revealed a main effect of treatment (t(df) = 2.564(22), $p = 0.0089$; mean ± SEM: AAV-GFP = 31.64 ± 1.212; AAV-GLT-1 = 39.09 ± 2.641). *t*-tests on NeuN immunoreactivity in S. pyramidale of CA1, S. pyramidale CA3, and the dentate gyrus for hippocampi both ipsilateral (Fig. 9) and contralateral (Fig. 10) to injection 30 days post-IHKA revealed no effect of treatment ($p > 0.05$) suggesting that pretreatment with an AAV-Gfa2-GLT-1-cHA viral vector is neuroprotective at early time points in epileptogenesis but does not prevent neurotoxicity in chronic stages in epileptogenesis.

3.4. Effects of AAV-GLT-1 on granule cell dispersion (GCD) during epileptogenesis

For GCD, we analyzed the width of the granule cell layer normalized to the contralateral hippocampus at 7 and 30 days post-IHKA-induced SE in AAV-Gfa2-GFP and AAV-Gfa2-GLT-1-cHA pretreated mice (Fig. 11, Fig. 12). A one-tailed *t*-test on GCL width at 7 days post-IHKA revealed a main effect of treatment (t(df) = 3.285(22), $p = 0.0017$; mean ± SEM: AAV-GFP = 123.9 ± 8.819; AAV-GLT-1 = 89.52 ± 5.622) (Fig. 11). A *t*-test on GCL width at 30 days post-IHKA revealed no effect of treatment ($p > 0.05$) (Fig. 12).

3.5. Pretreatment with AAV-GLT-1 suppresses total seizure time (TST) and large behavioral seizures (LBSs)

Electrographic seizure and large behavioral seizure (LBS) analysis was performed at 7 days post-IHKA induced SE in AAV-Gfa2-GFP and AAV-Gfa2-GLT-1 pretreated mice (Fig. 13, Supplemental Fig. S2). A one-tailed t-test on seizure frequency per hour at 7 days post-IHKA revealed a main effect of treatment (t(df) = 2.223(9), $p = 0.0266$; mean ± SEM: AAV-GFP = 2.136 ± 1.120; AAV-GLT-1 = 0.3274 ± 0.04839). A one-tailed t-test on average seizure duration at 7 days post-IHKA revealed no effect of treatment. A one-tailed t-test on total seizure time (TST) at 7 days post-IHKA revealed a main effect of treatment (t(df) = 2.961(9), $p = 0.0080$; mean ± SEM: AAV-GFP = 500.00 ± 197.6; AAV-GLT-1 = 74.58 ± 10.23). Electrographic events ≥20 s categorized as long events were further examined for presence of large behavioral seizures (LBSs). A one-tailed t-test on long event frequency at 7 days post-IHKA revealed a main effect of treatment (t(df) = 3.308(9), $p = 0.0046$; mean ± SEM: AAV-GFP = 4.250 ± 1.377; AAV-GLT-1 = 0.7143 ± 0.0.2857) (Fig. 13). A Mann-Whitney *U* test on LBSs ≥20 s at 7 days post-IHKA induced SE revealed LBSs were significantly decreased in AAV-GLT-1 pretreated mice (Mdn = 0.00) compared to AAV-GFP pretreated mice (Mdn = 1.500), U = 3.500, $p = 0.0242$ (Supplemental Fig. S2, Video 1, Video 2). No LBSs ≥20 s were observed in AAV-Gfa2-GLT-1 pretreated mice at 7 days post-IHKA induced SE (Supplemental Fig. S2).

4. Discussion

In this study, we used Western blot analysis, immunohistochemistry, and long-term-video-EEG monitoring to demonstrate that cell-type-specific upregulation of GLT-1 in astrocytes is neuroprotective at early time points during epileptogenesis, reduces total time spent in seizures and eliminates large behavioral seizures in the IHKA model of epilepsy. This is the first paper to demonstrate that astrocyte-specific upregulation of GLT-1 using an AAV viral vector is therapeutic in a preclinical model of epilepsy.

We have previously determined that crude synaptosomal GLT-1 levels, transporter readily available for glutamate uptake near glutamatergic synapses, are significantly downregulated at a critical time

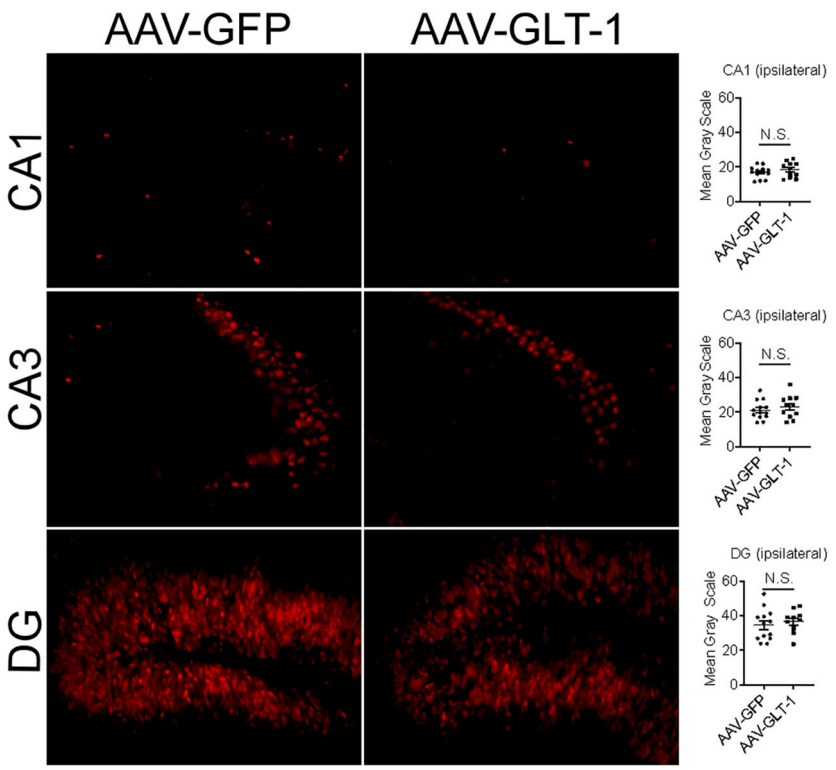

Fig. 9. NeuN expression in AAV pretreated mice in the ipsilateral hippocampus 30 days post-kainate induced status epilepticus. Coronal section of the ipsilateral hippocampus 30 days post-kainate induced status epilepticus showing expression and quantitation of NeuN immunoreactivity following AAV injection. AAV-GFP group; $N = 13$ sections (7 animals). AAV-GLT-1 group; $N = 11$ sections (6 animals) (20×).

point during the development of epilepsy (Peterson and Binder, 2019b). Clarkson et al., 2020 also found that there was a significant reduction in perisynaptic GLT-1 at the plasma membrane in astrocytes during the latent period following systemic KA-induced SE (Clarkson et al., 2020). Our current findings indicate that intrahippocampal AAV8-Gfa2-GLT-1 infusion selectively upregulates GLT-1 in GFAP-positive cells. Interestingly, a previous study showed that bilateral infusion of AAV9-EAAT2 did not have antiepileptic or neuroprotective effects (Young et al., 2014). An important distinction being the AAV viral vector used in our studies is 10-fold higher than the titer used in Young et al., 2014. This group did not observe an increase in EAAT expression with AAV vector infusion when comparing non-injected with AAV9-EAAT2 injected mice. Similarly, we did not observe a significant difference in GLT-1 expression between AAV-Gfa2-GFP and AAV-Gfa2-GLT-1 injected mice 12 days post-AAV injection (data not shown), but when mice injected with the two viral vectors were challenged with kainic acid, we observed a significant increase in GLT-1 expression in the ipsilateral hippocampus suggesting that AAV-GLT1_cHA injected mice have increased glutamate uptake compared to control mice injected with AAV-Gfa2-GFP. These findings could be due to an increase in exogenous GLT-1 produced under the GFAP promoter in response to increased astrogliosis post-kainate-induced SE in AAV-Gfa2-GLT1_cHA injected mice. We have previously demonstrated that GFAP immunoreactivity is upregulated in both hippocampi following kainic acid injection (Hubbard et al., 2016). Interestingly, we observed increased GLT-1 expression in the ipsilateral hippocampus at early and chronic time points in epileptogenesis, suggesting that the AAV GLT-1-cHA transgene is still being expressed at least five-week following infusion. Future studies could further investigate the function of these transporters during early and chronic phases of epileptogenesis by performing glutamate uptake assays on crude synaptosomes from mice injected with both viruses. We hypothesize that crude synaptosomal uptake studies would demonstrate increased uptake in the ipsilateral hippocampus of mice pretreated with AAV-Gfa2-GLT-1.

Second, we found that pretreatment with AAV8-Gfa2-GLT-1 delays neuronal death and granule cell dispersion at early time points in epileptogenesis but does not prevent neurotoxicity in chronic stages of epileptogenesis. A hallmark pathological feature of TLE is hippocampal sclerosis which includes dentate cell dispersion, neuronal cell loss, and gliosis, which are all observed in the IHKA model of epilepsy (Rusina et al., 2021; Thom, 2014). Mice infused with AAV-Gfa2-GLT-1 had significantly higher NeuN expression in CA3 and DG in the ipsilateral hippocampus compared to mice infused with control virus AAV-Gfa2-GFP. These data suggest that upregulation of GLT-1 is sufficient to delay neuronal loss at early time points following kainic acid-induced SE. In the hippocampus, widespread neuronal cell loss occurs in CA1, CA3, and the dentate gyrus hilus associated with mTLE (Scharfman and Pedley, 2007). CA1 hippocampal neuronal loss was observed in the ipsilateral hippocampus of mice pretreated with both viruses suggesting that over-expression of GLT-1 was not sufficient to prevent pyramidal neuronal loss in CA1. We also observed a significant increase in NeuN expression in the dentate gyrus of AAV-Gfa2-GLT-1 infused mice in the contralateral hippocampus compared to mice infused with control virus AAV-Gfa2-GLT-1. The occurrence of neurochemical modulation in the contralateral hippocampus has been observed following unilateral injection of kainic acid. Following unilateral injections of kainic acid, delayed neuronal death and astrogliosis are observed in the contralateral hippocampus (Hubbard et al., 2016; Magloczky and Freund, 1995). Our data suggest that although GLT-1 upregulation is localized to the ipsilateral hippocampus, it contributes to neuroprotection in the contralateral hippocampus at early time points in epileptogenesis. Although most seizures originate in the ipsilateral hippocampus, seizures can propagate to the contralateral hippocampus (Riban et al., 2002). These data suggest that although virally expressed GLT-1 is localized to the ipsilateral hippocampus, this additionally leads to protection in the contralateral hippocampus. The neuroprotection observed in the contralateral hippocampus at early time points in epileptogenesis

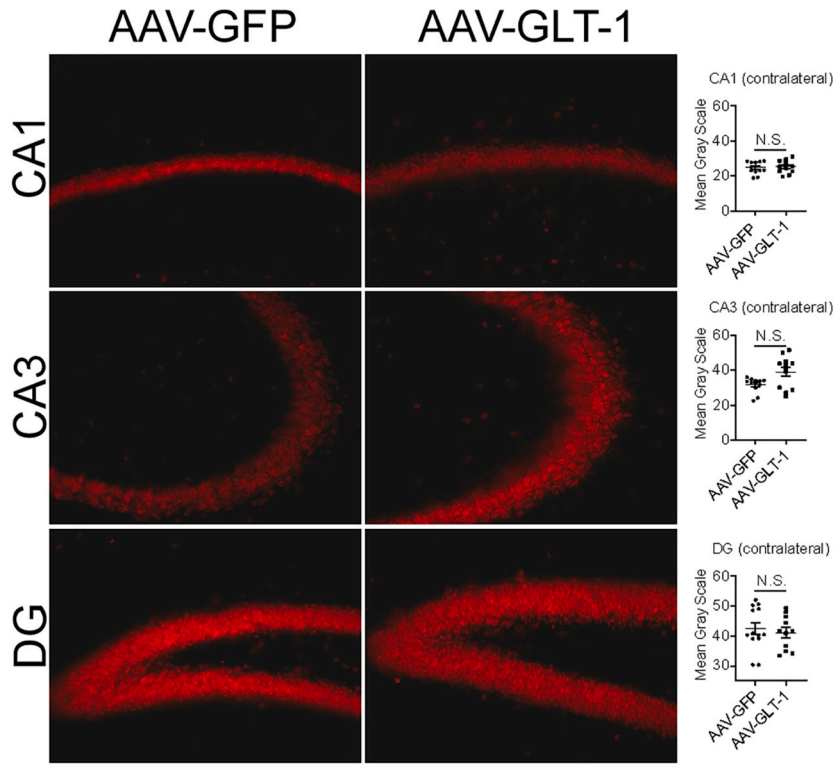

Fig. 10. NeuN expression in AAV pretreated mice in the contralateral hippocampus 30 days post-kainate induced status epilepticus. Coronal section of the contralateral hippocampus 30 days post-kainate induced status epilepticus showing expression and quantitation of NeuN immunoreactivity following AAV injection. AAV-GFP group; $N = 13$ sections (7 animals). AAV-GLT-1 group; $N = 11$ sections (6 animals) (20×).

could result from less seizure propagation to the contralateral hippocampus. Further studies could confirm this by recording epileptiform activity from both hippocampi. In contrast, pretreatment with AAV-Gfa2-GLT-1 did not prevent neurotoxicity at late time points during chronic phases of epileptogenesis. Therefore, the likely explanation is that overexpression of GLT-1 was sufficient to delay neuronal loss but did not protect against neuronal excitotoxicity at chronic time points in epilepsy.

Third, we determined that pre-treatment with AAV-Gfa2-GLT-1 reduces seizure frequency at seven days post-IHKA induced SE. Astrocyte-specific upregulation of GLT-1 did not prevent spontaneous seizures but significantly reduced the frequency of seizures compared to mice pretreated with control virus. In addition, initial SE-induced mortality was slightly reduced in AAV-GLT-1 pretreated mice (13%) compared with AAV-GFP pretreated mice (18%). Fourth, we determined that pretreatment with AAV8-Gfa2-GLT-1 reduces total seizure time at seven days post-IHKA induced SE. Total seizure time is the amount of time an animal spends having ictal activity that is classified as a seizure. Mice pretreated with AAV-Gfa2-GLT-1 spent significantly less time in seizures than mice pretreated with control virus AAV-Gfa2-GFP. Interventions

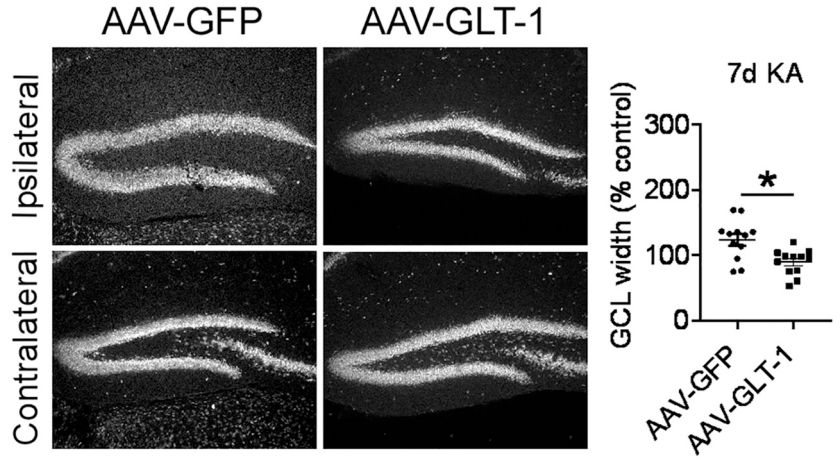

Fig. 11. NeuN expression showing granule cell dispersion in the hippocampus 7 days post-kainate induced status epilepticus . Coronal section of the ipsilateral hippocampus 7 days post-kainate induced status epilepticus showing expression of NeuN and comparison of granule cell layer width, normalized to contralateral hippocampus from the same section. $N = 12$ sections per group (6 animals per group) (10×).

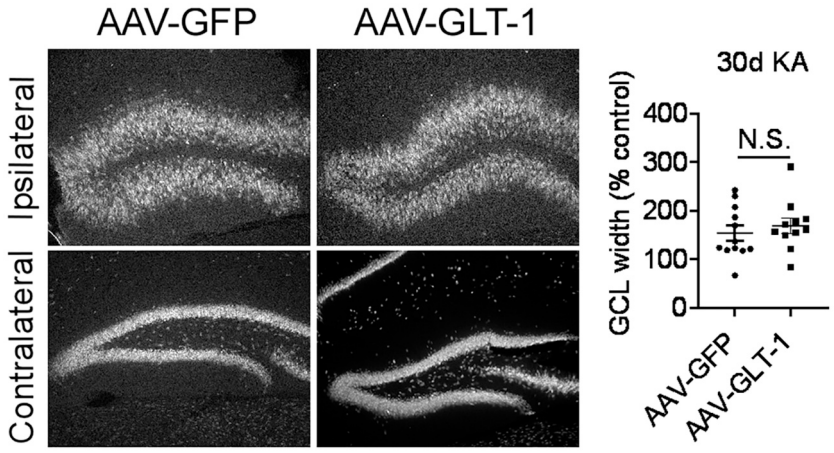

Fig. 12. NeuN expression showing granule cell dispersion in the hippocampus 30 days post-kainate induced status epilepticus. Coronal section of the ipsilateral hippocampus 30 days post-kainate induced status epilepticus showing expression of NeuN and comparison of granule cell layer width, normalized to contralateral hippocampus from the same section. AAV-GFP group; $N = 12$ sections (6 animals). AAV-GLT-1 group; $N = 11$ sections (6 animals) (10×).

that reduce seizure activity have been shown to improve behavioral outcomes (Falcicchia et al., 2018; Luo et al., 2021; Ramandi et al., 2021). Future studies could determine whether selective upregulation of GLT-1 in astrocytes improves cognitive performance in TLE. Fifth, we determined that pretreatment with AAV8-Gfa2-GLT-1 decreased the number of seizures ≥20 s and elminates long-duration large behavioral seizures. These data suggest that overexpression of GLT-1 using a viral vector in the ipsilateral hippocampus of IHKA mice is sufficient to reduce time spent in ictal activity. Interestingly, we did not observe a significant difference in seizure duration between treatment groups, but we did observe a significant reduction in long events in animals pretreated with AAV-Gfa2-GLT-1. We hypothesize that increased glutamate uptake through astrocytic GLT-1 is neuroprotective in both seizure initiation and termination. We did not observe long duration LBSs in mice pretreated with AAV-Gfa2-GLT-1. GLT-1 could be playing a crucial role in seizure termination, which is critical in preventing the life-threatening condition status epilepticus (Betjemann and Lowenstein, 2015). Thus, hippocampal upregulation of GLT-1 may prevent seizures from spreading outside the hippocampus, which would explain the lack of motor seizures in the AAV-Gfa2-GLT-1 treated group **(**Supplemental Fig. S2**).**

Several preclinical studies have suggested that targeting GLT-1 overexpression could be therapeutic in many neurological diseases, including epilepsy (Chotibut et al., 2014; Chotibut et al., 2017; Hussein et al., 2016; Ramandi et al., 2021; Sari et al., 2010; Sha et al., 2016; Zeng et al., 2010). Ceftriaxone, a β-lactam antibiotic, has been shown to increase GLT-1 expression at early time points in epileptogenesis and might reduce cognitive impairments observed in epilepsy but how ceftriaxone increases glutamate uptake is unclear (Hussein et al., 2016; Ramandi et al., 2021). Previous studies have indicated that GLT-1 mRNA is upregulated with ceftriaxone administration, while some studies suggest that ceftriaxone does not increase the expression of GLT-1 (Griffin et al., 2021; Ramandi et al., 2021). Ceftriaxone treatment has also been shown to impair synaptic plasticity in the hippocampus and impair memory recognition, suggesting that ceftriaxone could affect other pathways in the CNS (Matos-Ocasio et al., 2014; Omrani et al., 2009). These data suggest that targeting glutamate uptake could be an alternative treatment to reduce seizures and reveal the importance of a selective modulator of GLT-1. Recently, a novel allosteric modulator of GLT-1, GT949, was shown to have promising results in selectively increasing the activity of GLT-1 *in vitro* (Falcucci et al., 2019). Further studies need to be performed to test the efficacy of this compound *in vivo*. The ideal therapeutic agent would be an orally active drug that crosses the BBB and modulates GLT-1 over the epileptogenic susceptibility period after a given insult. 20 mM kainic acid to induce SE is a substantial insult to the hippocampus, therefore in this model we hypothesize that the AAV-Gfa2-GLT-1 can only delay the neurotoxicity. In future studies, dose and frequency of GLT-1 upregulation could be therapeutically tailored to the severity of insult.

Post-translational modifications (PTMs) of GLT-1 including palmitoylation, ubiquitination, nitrosylation and sumoylation regulate transporter activity and cellular localization (Peterson and Binder, 2019a). Dysregulation of GLT-1 has been observed across many neurological diseases including epilepsy while mislocalization and internalization of this transporter in the cell membrane could be due to aberrant PTMs. For example, inhibition of GLT-1 palmitoylation leads to approximately a 30% reduction in glutamate uptake suggesting that palmitoylation of the transporter is important for its function (Huang et al., 2010). In a mouse model of Huntington's disease (HD), GLT-1 palmitoylation is reduced significantly which could be contributing to the decreased glutamate uptake observed in this model. The ubiquitination/deubiquitination of GLT-1 is also important for trafficking of the transporter to and from the plasma membrane. The laforin/malin complex, which works as an E3 ubiquitin ligase, is thought to play an important role in the retention of GLT-1 at the plasma membrane while Nedd4–2, another ubiquitin ligase, has been shown to mediate the internalization and degradation of GLT-1 (Garcia-Tardon et al., 2012). GLT-1 expression is decreased in the midbrain and striatum in the 1-methyl-4-phenyl-1,2,3,6-tetrahydropyridine (MPTP) mouse model of Parkinson's disease (PD). Interestingly, knocking down Nedd4–2 in this model of PD rescued GLT-1 protein levels (Zhang et al., 2017). Lafora disease, a genetic form of epilepsy, is caused by a mutation in EPM2A (encodes laforin) or EPM2B (encodes malin). In Lafora disease, ubiquitination of astrocytic GLT-1 is decreased and expression of the transporter at the cell membrane is significantly reduced which could be contributing to the refractory seizures observed in this disease (Munoz-Ballester et al., 2016; Perez-Jimenez et al., 2021). Targeting proteins that are important in the trafficking of GLT-1, like laforin, could lead to novel therapeutics for numerous neurological diseases. GLT-1 is expressed in perisynaptic astrocytic processes (PAPs) at high levels (Furness et al., 2008; Schreiner et al., 2014).

In summary, we report the first evaluation of an AAV8-Gfa2-GLT-1 viral vector in the IHKA model of epilepsy. Our findings provide evidence that glutamate uptake modulation can be therapeutically targeted for the attenuation of epilepsy. We demonstrate that overexpression of astrocytic GLT-1 has both antiepileptic and anti-seizure effects.

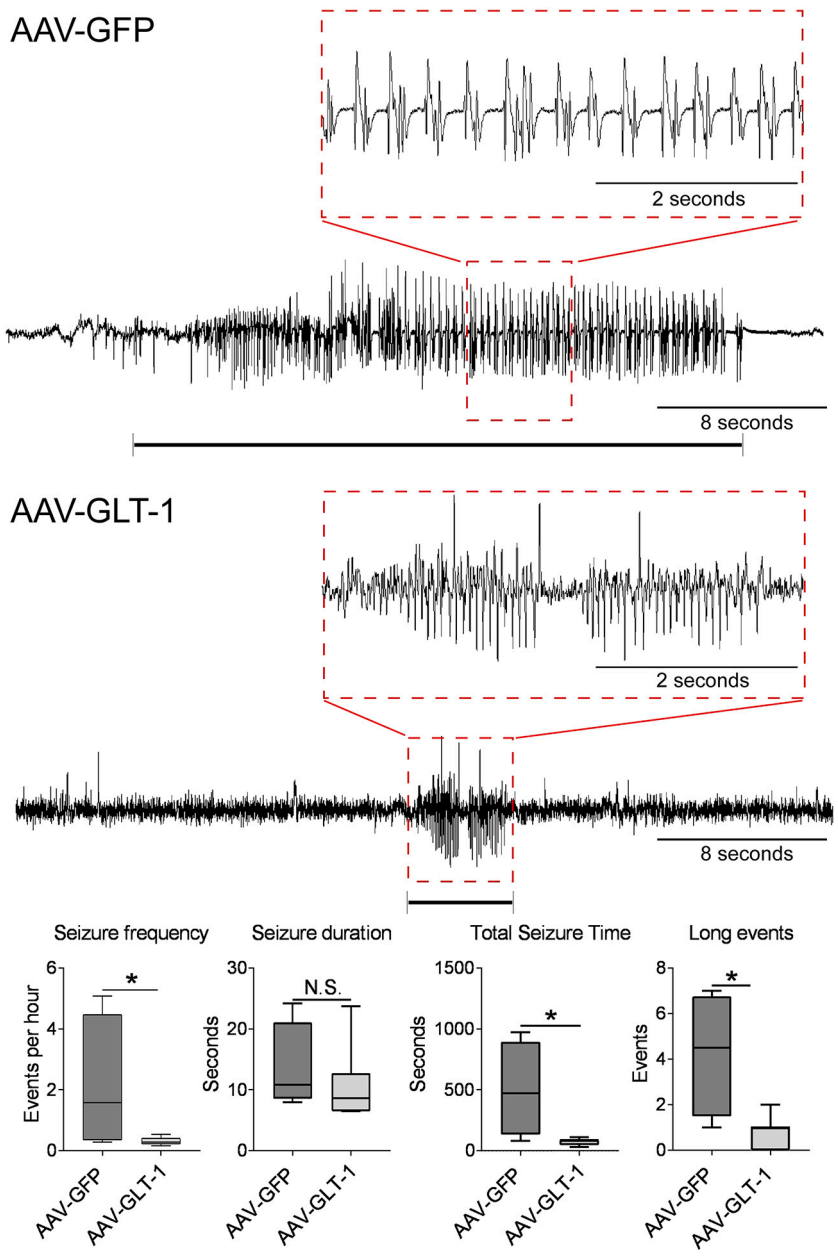

Fig. 13. Electrographic seizure burden in AAV pretreated mice post-IHKA induced status epilepticus. Representative EEG trace at 7 days post-kainate induced SE in AAV-GFP *vs.* AAV-GLT-1 pretreated mice. Graphs show seizure events per hour, average seizure duration, total seizure time and long events at 7 days post-IHKA induced status epilepticus (AAV-GFP: $N = 4$, AAV-GLT-1 $N = 7$).

Targeting astrocyte glutamate uptake could be useful in treating patients that are refractory to currently available antiepileptic drugs.

Supplementary data to this article can be found online at https://doi.org/10.1016/j.nbd.2021.105443.

Author contributions

ARP and DKB co-wrote the manuscript and designed experiments. ARP, TAG, and SKTW performed experiments and analyzed the results. KC and EVP modified and extended an expanded graphical user interface (GUI) from a previously published and validated MATLAB algorithm for automated electrographic seizure detection.

Funding

This research did not receive any specific grant from funding agencies in the public, commercial, or not-for-profit sectors.

Declaration of Competing Interest

The authors declare no competing interests.

Acknowledgements

The authors would like to thank Dr. Meera Nair, Dr. Declan McCole and Dr. Djurdjica Coss (UCR) for the use of their Leica DM5500 fluorescence microscope and Carrie Jonak for breeding the mice used for this study.

References

Asadi-Pooya, A.A., et al., 2017. Prevalence and incidence of drug-resistant mesial temporal lobe epilepsy in the United States. World Neurosurg. 99, 662–666.

Betjemann, J.P., Lowenstein, D.H., 2015. Status epilepticus in adults. Lancet Neurol. 14, 615–624.

Binder, D.K., 2018. Astrocytes: stars of the sacred disease. Epilepsy Curr. 18, 172–179.

Bootsma, H.P., et al., 2009. The impact of side effects on long-term retention in three new antiepileptic drugs. Seizure. 18, 327–331.

Chotibut, T., et al., 2014. Ceftriaxone increases glutamate uptake and reduces striatal tyrosine hydroxylase loss in 6-OHDA Parkinson's model. Mol. Neurobiol. 49, 1282–1292.

Chotibut, T., et al., 2017. Ceftriaxone reduces L-dopa-induced dyskinesia severity in 6-hydroxydopamine parkinson's disease model. Mov. Disord. 32, 1547–1556.

Clarkson, C., et al., 2020. Ultrastructural and functional changes at the tripartite synapse during epileptogenesis in a model of temporal lobe epilepsy. Exp. Neurol. 326, 113196.

Consortium, E. K, 2016. De novo mutations in SLC1A2 and CACNA1A are important causes of epileptic encephalopathies. Am. J. Hum. Genet. 99, 287–298.

Danbolt, N.C., 2001. Glutamate uptake. Prog. Neurobiol. 65, 1–105.

Eid, T., et al., 2004. Loss of glutamine synthetase in the human epileptogenic hippocampus: possible mechanism for raised extracellular glutamate in mesial temporal lobe epilepsy. Lancet. 363, 28–37.

Falcicchia, C., et al., 2018. Seizure-suppressant and neuroprotective effects of encapsulated BDNF-producing cells in a rat model of temporal lobe epilepsy. Mol Ther. Methods Clin. Dev. 9, 211–224.

Falcucci, R.M., et al., 2019. Novel positive allosteric modulators of glutamate transport have neuroprotective properties in an in vitro excitotoxic model. ACS Chem. Neurosci. 10, 3437–3453.

Falnikar, A., et al., 2016. GLT1 overexpression reverses established neuropathic pain-related behavior and attenuates chronic dorsal horn neuron activation following cervical spinal cord injury. Glia. 64, 396–406.

Fedele, D.E., et al., 2005. Astrogliosis in epilepsy leads to overexpression of adenosine kinase, resulting in seizure aggravation. Brain. 128, 2383–2395.

Fisher, R.S., et al., 2014. ILAE official report: a practical clinical definition of epilepsy. Epilepsia. 55, 475–482.

Furness, D.N., et al., 2008. A quantitative assessment of glutamate uptake into hippocampal synaptic terminals and astrocytes: new insights into a neuronal role for excitatory amino acid transporter 2 (EAAT2). Neuroscience. 157, 80–94.

Garcia-Tardon, N., et al., 2012. Protein kinase C (PKC)-promoted endocytosis of glutamate transporter GLT-1 requires ubiquitin ligase Nedd4-2-dependent ubiquitination but not phosphorylation. J. Biol. Chem. 287, 19177–19187.

Griffin, W.C., et al., 2021. Effects of ceftriaxone on ethanol drinking and GLT-1 expression in ethanol dependence and relapse drinking. Alcohol. 92, 1–9.

Harvey, B.K., et al., 2011. Targeted over-expression of glutamate transporter 1 (GLT-1) reduces ischemic brain injury in a rat model of stroke. PLoS One 6, e22135.

Heuser, K., et al., 2018. Ca2+ signals in astrocytes facilitate spread of epileptiform activity. Cereb. Cortex 28, 4036–4048.

Hinterkeuser, S., et al., 2000. Astrocytes in the hippocampus of patients with temporal lobe epilepsy display changes in potassium conductances. Eur. J. Neurosci. 12, 2087–2096.

Huang, K., et al., 2010. Palmitoylation and function of glial glutamate transporter-1 is reduced in the YAC128 mouse model of Huntington disease. Neurobiol. Dis. 40, 207–215.

Hubbard, J.A., et al., 2016. Regulation of astrocyte glutamate transporter-1 (GLT1) and aquaporin-4 (AQP4) expression in a model of epilepsy. Exp. Neurol. 283, 85–96.

Hussein, A.M., et al., 2016. Beta lactams antibiotic ceftriaxone modulates seizures, oxidative stress and connexin 43 expression in hippocampus of pentylenetetrazole kindled rats. J. Epilepsy. Res. 6, 8–15.

Ivens, S., et al., 2007. TGF-beta receptor-mediated albumin uptake into astrocytes is involved in neocortical epileptogenesis. Brain. 130, 535–547.

Kong, Q., et al., 2012. Increased glial glutamate transporter EAAT2 expression reduces epileptogenic processes following pilocarpine-induced status epilepticus. Neurobiol. Dis. 47, 145–154.

Lee, D.J., et al., 2012. Decreased expression of the glial water channel aquaporin-4 in the intrahippocampal kainic acid model of epileptogenesis. Exp. Neurol. 235, 246–255.

Liu, Y., et al., 2015. Short-term use of antiepileptic drugs is neurotoxic to the immature brain. Neural Regen. Res. 10, 599–604.

Luo, X.M., et al., 2021. Post-status epilepticus treatment with the Fyn inhibitor, saracatinib, improves cognitive function in mice. BMC Neurosci. 22, 2.

Magloczky, Z., Freund, T.F., 1995. Delayed cell death in the contralateral hippocampus following kainate injection into the CA3 subfield. Neuroscience. 66, 847–860.

Mathern, G.W., et al., 1999. Hippocampal GABA and glutamate transporter immunoreactivity in patients with temporal lobe epilepsy. Neurology. 52, 453–472.

Matos-Ocasio, F., et al., 2014. Ceftriaxone, a GLT-1 transporter activator, disrupts hippocampal learning in rats. Pharmacol. Biochem. Behav. 122, 118–121.

Munoz-Ballester, C., et al., 2016. Homeostasis of the astrocytic glutamate transporter GLT-1 is altered in mouse models of Lafora disease. Biochim. Biophys. Acta 1862, 1074–1083.

Omrani, A., et al., 2009. Up-regulation of GLT-1 severely impairs LTD at mossy fibre–CA3 synapses. J. Physiol. 587, 4575–4588.

Park, S.P., Kwon, S.H., 2008. Cognitive effects of antiepileptic drugs. J. Clin. Neurol. 4, 99–106.

Perez-Jimenez, E., et al., 2021. Endocytosis of the glutamate transporter 1 is regulated by laforin and Malin: implications in Lafora disease. Glia. 69, 1170–1183.

Peterson, A.R., Binder, D.K., 2019a. Post-translational regulation of GLT-1 in neurological diseases and its potential as an effective therapeutic target. Front. Mol. Neurosci. 12, 164.

Peterson, A.R., Binder, D.K., 2019b. Regulation of synaptosomal GLT-1 and GLAST during epileptogenesis. Neuroscience. 411, 185–201.

Peterson, A.R., Binder, D.K., 2020. Astrocyte glutamate uptake and signaling as novel targets for antiepileptogenic therapy. Front. Neurol. 11, 1006.

Petr, G.T., et al., 2015. Conditional deletion of the glutamate transporter GLT-1 reveals that astrocytic GLT-1 protects against fatal epilepsy while neuronal GLT-1 contributes significantly to glutamate uptake into synaptosomes. J. Neurosci. 35, 5187–5201.

Racine, R.J., 1972. Modification of seizure activity by electrical stimulation. II. Motor seizure. Electroencephalogr. Clin. Neurophysiol. 32, 281–294.

Ramandi, D., et al., 2021. Pharmacological upregulation of GLT-1 alleviates the cognitive impairments in the animal model of temporal lobe epilepsy. PLoS One 16, e0246068.

Riban, V., et al., 2002. Evolution of hippocampal epileptic activity during the development of hippocampal sclerosis in a mouse model of temporal lobe epilepsy. Neuroscience. 112, 101–111.

Rusina, E., et al., 2021. The kainic acid models of temporal lobe epilepsy. eNeuro. 8.

Sari, Y., et al., 2010. Ceftriaxone-induced up-regulation of cortical and striatal GLT1 in the R6/2 model of Huntington's disease. J. Biomed. Sci. 17, 62.

Scharfman, H., Pedley, T., 2007. Temporal lobe epilepsy. In: Gilman, S. (Ed.), The Neurobiology of Disease. Academic Press, New York, NY, pp. 349–370.

Schreiner, A.E., et al., 2014. Laminar and subcellular heterogeneity of GLAST and GLT-1 immunoreactivity in the developing postnatal mouse hippocampus. J. Comp. Neurol. 522, 204–224.

Sha, L., et al., 2016. Pharmacologic inhibition of Hsp90 to prevent GLT-1 degradation as an effective therapy for epilepsy. In: Wu, L. (Ed.), The Journal of Experimental Medicine, Vol. 214, pp. 547–563.

Tanaka, K., et al., 1997. Epilepsy and Exacerbation of Brain Injury in Mice Lacking the Glutamate Transporter GLT-1, 276, pp. 1699–1702.

Tessler, S., et al., 1999. Expression of the glutamate transporters in human temporal lobe epilepsy. Neuroscience. 88, 1083–1091.

Thom, M., 2014. Review: hippocampal sclerosis in epilepsy: a neuropathology review. Neuropathol. Appl. Neurobiol. 40, 520–543.

Young, D., et al., 2014. Adenosine kinase, glutamine synthetase and EAAT2 as gene therapy targets for temporal lobe epilepsy. Gene Ther. 21, 1029–1040.

Zack, M.M., Kobau, R., 2017. National and state estimates of the numbers of adults and children with active epilepsy - United States, 2015. MMWR Morb. Mortal. Wkly Rep. 66, 821–825.

Zeidler, Z., et al., 2018. Targeting the mouse ventral Hippocampus in the intrahippocampal kainic acid model of temporal lobe epilepsy. eNeuro. 5.

Zeng, L.H., et al., 2010. Modulation of astrocyte glutamate transporters decreases seizures in a mouse model of tuberous sclerosis complex. Neurobiol. Dis. 37, 764–771.

Zhang, Y., et al., 2017. Regulation of glutamate transporter trafficking by Nedd4-2 in a Parkinson's disease model. Cell Death Dis. 8, e2574.